Comparative Biochemistry and Physiology - Part D 29 (2019) 286–298

Contents lists available at ScienceDirect

Comparative Biochemistry and Physiology - Part D

journal homepage: www.elsevier.com/locate/cbpd

Genome-wide identification of the Na^+/H^+ exchanger gene family in *Lateolabrax maculatus* and its involvement in salinity regulation

Yang Liu, Haishen Wen, Xin Qi, Xiaoyan Zhang, Kaiqiang Zhang, Hongying Fan, Yuan Tian, Yanbo Hu, Yun Li*

Key Laboratory of Mariculture (Ocean University of China), Ministry of Education, Qingdao 266003, China

ARTICLE INFO

Keywords:
NHEs gene
Lateolabrax maculatus
Genome-wide
Salinity
Expression patterns

ABSTRACT

Na^+/H^+ exchangers (NHEs) are one of the major groups of transmembrane proteins that play crucial roles in pH homeostasis, cell volume regulation and Na^+ transport in animals. In our study, twelve *NHEs* were identified from transcriptomic and genomic databases of *Lateolabrax maculatus*. The evolutionary footprint of each *NHE* gene was revealed via the analysis of phylogenetic tree, copy numbers, exon-intron structures and motif compositions. *NHEs* harbored a high proportion of α-helices (54.7% to 67.0%) and a low proportion of β-sheets (1.3%) and contained 9–13 transmembrane helices (TM). Results of tissue distribution detection revealed that *L. maculatus NHE* genes exhibited different expression profiles in a tissue-specific manner under normal physiological conditions. In the main osmoregulatory organ, gill, *NHE2c* and *NHE3* showed significant higher expression comparing with other *L. maculatus NHE* genes. To gain insight into the potential function of *L. maculatus NHE* genes in response to salinity changes, we evaluated their expression variation after different salinity treatment (0 ppt, 12 ppt, 30 ppt, 45 ppt). During acute salinity stress experiment, *L. maculatus NHE* genes were regulated in a gene-specific and time-dependent manner. Most *NHE* genes were upregulated to different extent by low salinity (0 ppt) and exhibited the highest expression value in gills at 6 h, while *NHE2c* and *NHE3* were the most strongly induced genes, suggesting they may play crucial roles in salinity and osmotic regulation. In addition, the expressions of several *NHE* genes were regulated by isotonic or high salinity treatments, indicating their potential involvements in response to salinity challenge. Our findings in this study provide a foundation for future studies about *NHE* gene deciphering stress physiology correlated to salinity and osmotic regulation in teleosts.

1. Introduction

Na^+/H^+ exchangers (NHEs), which are encoded by the SLC9 gene family of solute carrier classification of transporters (SLC), are ubiquitous ion transporters present from prokaryotes to eukaryotes (Hwang and Lee, 2007; Hwang et al., 2011). The SLC9 gene family encompasses three subgroups: SLC9A: Na^+/H^+ antiporters (*SLC9A1-9*, encoding NHE1-9); SLC9B: *SLC9B1* and *SLC9B2* encoding two recently cloned gene copies, NHA1 and NHA2, respectively; SLC9C: *SLC9C1*(sperm-specific NHE) and *SLC9C2* (Watanabe et al., 2008). NHEs are believed to play fundamental roles in pH homeostasis, cell volume regulation and Na^+ transport in animals. Compared with terrestrial animals, fish have to cope with more challenging aquatic environments caused by diverse salinities, pH values and ion compositions. Among all of the NHE genes, NHEs encoded by *SLC9A* (NHE1-9) are believed to play essential roles in transferring sodium and acid/base between the aquatic environment and the body of a fish (Musch et al., 2009). These NHEs can be categorized into two subgroups that are based on subcellular localization and phylogenic analysis: plasmalemmal NHEs (NHE1-5) and intracellular NHEs (NHE6-9) (Wagner et al., 2004). However, some recent studies demonstrate that NHE8 is not only expressed at the intracellular vesiculation but also at the apical membrane of the proximal tubule and intestine (Goyal et al., 2003; Hua et al., 2005). In fish species, NHE4 is missing from the genome sequence of zebrafish (*Danio rerio*) (Howe et al., 2013), medaka (*Oryzias latipes*) (Kasahara et al., 2007), and European sea bass (*Dicentrarchus labrax*) (Tine et al., 2014). Instead, an additional nonmammalian member *NHEβ* was found in the red blood cells (RBC) of some teleosts, such as rainbow trout (*Oncorhynchus mykiss*) and European flounder (*Platichthys flesus*), which can maintain the stability of RBC pH during a generalized acidosis (Rummer et al., 2010). Therefore, before investigating the roles of NHEs in specific species, it is critically important

* Corresponding author.
E-mail address: yunli0116@ouc.edu.cn (Y. Li).

https://doi.org/10.1016/j.cbd.2019.01.001
Received 8 November 2018; Received in revised form 3 January 2019; Accepted 4 January 2019
Available online 09 January 2019
1744-117X/ © 2019 Elsevier Inc. All rights reserved.

to determine the gene copies, gene structures and gene evolution of NHEs.

Studies about NHEs started in 1976 by Murer et al., in which the first NHE was isolated from the rat small intestine and kidney (Capasso et al., 2005). Since then, understanding of the details of the function and regulation of NHEs at the cellular and whole organism levels has increased, see reviewed paper in 2006 (Malo and Fliegel, 2006), 2013 (Donowitz et al., 2013) and 2014 (Fuster and Alexander, 2014). However, almost all of those studies were limited to mammalian species, whereas reports about NHEs in fish were far fewer. Evidence for fish NHEs comes from gene cloning, physiological analysis and immunohistochemical data. Among nonmammalian NHEs, *NHE2* and *NHE3* have received the most attention in fish osmoregulation research and have been cloned from several species, including Atlantic stingray (*Dasyatis Sabina*) (Choe et al., 2005), zebrafish (Yan et al., 2007), Mozambique tilapia (*Oreochromis mossambicus*) (Watanabe et al., 2008), rainbow trout (*Salmo irideus*) (Ivanis et al., 2008b), banded houndshark (*Triakis scyllium*) (Li et al., 2013), and Pacific dogfish (*Squalus suckleyi*) (Guffey et al., 2015). The *NHE2* and *NHE3* genes have been confirmed to be expressed in gill mitochondrion rich cells (MRCs), and their expression has been shown to increase by exposure to soft water in zebrafish (Yan et al., 2007), or in acclimation to freshwater (FW) conditions in euryhaline fish such as killifish (*Fundulus heteroclitus*) (Scott and Schulte, 2005). Gene-specific expression differences have been reported in rainbow trout: *NHE2* mRNA increased during hypercapnic acidosis, whereas *NHE3* did not (Ivanis et al., 2008a). In stingray *D. sabina* (Choe et al., 2005) and bull shark *Carcharhinus leucas* (Reilly et al., 2011), *NHE3* mRNA increased in brackish water versus seawater. In addition to the gill in elasmobranch species, such as *T. scyllium* (Li et al., 2013), *NHE3* was also detected in the kidney and intestine, and its expression changed along with different salinity environments. All of the evidence suggests the potential roles of *NHE2* and *NHE3* in branchial, renal and intestinal ion regulation. For other fish NHE members, only a few genes have been cloned but not been functionally analyzed; therefore, their features were largely unknown.

Spotted sea bass (*Lateolabrax maculatus*), as a euryhaline teleost that can survive in a wide range of salinity environments (from 0 ppt to 38 ppt) (X. Zhang et al., 2017), is an ideal model for salinity regulation-related studies. With the interest in understanding the *NHE* genes in the spotted sea bass genome and their involvement in response to salinity changes, we conducted the identification and annotation of *NHE* genes. In addition, their expression variations in different salinity treatments were determined, which provided insights into their roles in ion regulation and in the anti-stress mechanisms of *L. maculatus*.

2. Materials and methods

2.1. Ethics statement

All animal experiments were conducted in accordance with the guidelines and approval of the respective Animal Research and Ethics Committees of Ocean University of China (Permit Number: 20141201). The field studies did not involve endangered or protected species.

2.2. Identification of NHE genes in spotted sea bass

To identify *NHE* genes in spotted sea bass, the transcriptome databases (X. Zhang et al., 2017), and the whole genome sequence database (unpublished data) were searched using the query sequences generated from *NHE* members in humans (*Homo sapiens*), zebrafish and barramundi (*Lates calcarifer*) retrieved from the Ensembl (http://www.ensembl.org) and NCBI (http://www.ncbi.nlm.nih.gov/) databases. TBLASTN was performed to obtain the initial pool of *NHE* gene sequences with a cutoff *E*-value of 1e-5, and then a unique set of sequences were retained after removing the repeated entries for further analysis. The cDNA sequences retrieved from transcriptome databases were confirmed by comparisons with the whole genome sequence of spotted sea bass by using BLASTN with a cutoff *E*-value of 1e-10. Open reading frames (ORF) were determined by using the ORF finder (https://www.ncbi.nlm.nih.gov/orffinder/) and were validated by BLASTP against the NCBI non-redundant protein database. For genes retrieved from the whole genome sequence only (not existing in the transcriptomic database), Fgenesh from SoftBerry (http://linux1.softberry.com/all.htm) was used to predict the exon and amino acid sequences. The *L. maculatus NHE* genes were named following the ZFIN (Zebrafish Nomenclature Guidelines), and the nomenclature of already published species for those expanded genes (Hyndman et al., 2009; Harter et al., 2018). Copy numbers were compared based on the genome databases of spotted sea bass and several other vertebrates. The chromosomal location of each *NHE* gene was displayed according to their coordinates on the genome.

2.3. Phylogenetic and syntenic analyses of NHEs

The *NHE* amino acid sequences of spotted sea bass and several representative vertebrates were used to perform the phylogenetic analysis. The criteria for choosing those OTUs was that we selected model animals and teleosts with well annotated genomes. For fish species, we selected representative species including stenohaline and euryhaline species. Including those from human (*H. sapiens*), mouse (*Mus musculus*), chicken (*Gallus gallus*), common chimpanzee (*Pan troglodytes*), bonobo (*Pan paniscus*) and sooty mangabeys (*Cercocebus atys*), and correlative fish species including zebrafish (*D. rerio*), tilapia (*Oreochromis niloticus*), medaka, fugu (*Takifugu rubripes*), barramundi (*L. calcarifer)*, large yellow croaker (*Larimichthys crocea*), Japanese flounder (*Paralichthys olivaceus*), ballan wrasse (*Labrus bergylta*), amberjack (*Seriola dumerili*) and bicolor damselfish (*Stegastes partitus*), their accession numbers were presented in Supplementary Table 1. After conducting multiple alignments of *NHE* sequences by MUSCLE (Edgar, 2004), Poisson model in MEGA 7 (Kumar et al., 2016) was used to evaluate the phylogenetic relationships of all *NHEs*. Neighbor-joining (NJ) phylogenetic trees were built with 1000 bootstrap replications. The tree was displayed with Interactive Tree Of Life (iTOL, http://itol.embl.de/).

To provide further confirmation of gene orthologs, syntenic analysis was performed for *NHE* members of spotted sea bass that are not well supported by the phylogenetic tree. Synteny blocks were built by comparing the genome regions around the *NHEs* between spotted sea bass and several other vertebrates. The positional information of neighboring genes in *L. maculatus NHEs* were extracted from the whole genome annotations, whereas other vertebrates were obtained from related NCBI and Ensemble databases.

2.4. Sequence analyses of NHEs

According to the deduced amino acids composition, protein characteristics were predicted by the Prot Param tool (Gasteiger et al., 2003), (http://www.expasy.ch/tools/protparam.html). The program of TMHMM (v.2.0) (http://www.cbs.dtu.dk/services/TMHMM/) estimated the probability of forming a transmembrane helix (TM) in *NHEs* (Krogh et al., 2001). The homologous domain architectures of the *NHE* genes in spotted sea bass were generated by the SMART 7.0 program (Letunic et al., 2012), (http://smart.embl.de/smart/). The exon-intron structures of *NHEs* were obtained from the *L. maculatus* database and were visualized using the GSDS software (Hu et al., 2015), (http://gsds.cbi.pku.edu.cn). The conserved motifs of *NHE* proteins were observed with MEME software (Brown et al., 2013), (http://meme.nbcr.net/meme/), and the optimum widths of motifs were set as 6–50 amino acids. According to the domain positions and with statistical significance (*E*-value less than E-40), 12 was selected as the maximum number of motifs; all of the other parameters were set at default. The predicted motifs of *NHE* proteins were further annotated by searching

the InterProScan database (Mulder and Apweiler, 2007), (http://www.ebi.ac.uk/Tools/pfa/iprscan). Furthermore, the three-dimensional protein structures of *L. maculatus NHEs* were systematically constructed by the Swiss Model software (http://swissmodel.expasy.org/), and the corresponding spatial images were depicted by Swiss-Pdb Viewer 4.1.0 (N and MC, 1997).

2.5. Salinity challenge and sample preparation

To examine the tissue distribution of *NHE* mRNA, spotted sea bass (1.64 ± 0.29 kg) were purchased from Haifa fishing farm (Qingdao, China) and then were dissected under anesthesia by tricaine methane sulfonate (MS 222, 200 mg/L). The skin, gill, kidney, intestine, liver, stomach, gonad, spleen, heart, brain, muscle and pituitary were collected. Then the samples were quickly frozen by liquid nitrogen and subsequently were stored at −80 °C for RNA extraction.

To determine the expression patterns of *NHE* genes in response to different salinities, the salinity challenge experiment was carried out in Shuangying Aquatic Seedling Co., Ltd., lijin, Shandong, China. Fish were temporarily reared in cultured salinity of 30 ppt for one week, under appropriate abiotic conditions (temperature: 24 ± 1 °C, dissolved oxygen: 7.0 ± 0.5 mg/L, pH: 7.8 ± 0.4). After acclimation, 96 spotted sea bass fingerlings (80.66 ± 13.05 g) were immediately transferred to 12 tanks with different water salinities, including low salinity (0 ppt), isotonic point salinity (12 ppt), control salinity group (30 ppt) and high salinity group (45 ppt), and all treatment groups were performed in triplicates. Before salinity experiment, the gills of six fish fingerlings with similar size were collected as 0 h samples. The sampling times were 6, 12, 24 and 72 h after transferring to different salinity groups, and the gills of six fish from each treatment were collected and pooled together as three mixed samples (two fish per tank) in each sampling time. The samples were frozen in liquid nitrogen and stored at −80 °C for RNA extraction.

2.6. Quantification of the mRNA expression

The total RNA for each sample was extracted using RNAiso reagent (Takara, Otsu, Japan) according to the manufacturer's protocol. gDNA was removed by using a PrimeScript RT reagent kit (Takara). The concentration and integrity of extracted RNAs were examined by using the Biodropsis BD-1000 nucleic acid analyzer (OSTC, Beijing) and electrophoresis. First-strand cDNA was synthesized using Reverse Transcriptase M-MLV (Takara). Quantitative real-time PCR (qRT-PCR) was performed to detect the expression levels of *NHE* mRNA, and the primers used in this paper were designed by Primer 5 software (Table 1). *18S* mRNA was used as the internal control to calibrate the qRT-PCR veracity and the samples were run in triplicate. Each 20-μL qRT-PCR reaction system contained 2 μL template cDNA, 0.4 μL each forward/reverse primer, 10 μL SYBR®FAST qPCR Master Mix (2×), 0.4 μL ROX, and 6.8 μL of nuclease-free water. qRT-PCR was performed in a 96-well optical plate at 95 °C for 30 s, followed by 40 cycles at 95 °C for 5 s and Tm for 30 s. Using the StepOne Plus Real-Time PCR system (Applied Bio systems), and the relative mRNA expression levels of genes were calculated according to the comparative $2^{-\Delta\Delta CT}$ method.

One-way (ANOVA) and Duncan's multiple range tests were performed to evaluate the difference degree among various treatments by SPSS 21.0. Differences were considered as statistical significance when $P < 0.05$. The graphs were depicted by the software of OriginPro 9.0.

3. Results

3.1. Identification and chromosomal distribution of NHE genes

A total of 12 *NHE* genes were identified in the *L. maculatus* genome and were named according to the nomenclature, including *NHEβ*, *NHE1*, *NHE2a*, *NHE2b*, *NHE2c*, *NHE3*, *NHE5*, *NHE6a*, *NHE6b*, *NHE7*, *NHE8* and *NHE9*. All *NHEs* cDNA sequences were submitted to GenBank, and their accession numbers and protein characteristics were presented in Table 2. The predicted *NHE* proteins have amino acid numbers from 599 to 980, molecular weights (Mw) from 65.0 to 107.0 kD, and isoelectric points ranging from 5.33 to 8.88.

Table 1
Primers used for quantitative RT-PCR of *NHE* genes.

Gene	Primer sequence(5′-3′)
NHEbeta	
F	CAGGAAACCAAGGGAGA
R	ACAAGTTCCGCATCGTC
NHE1	
F	AGAAGCCAACTGCTGCCAAG
R	CAGCCTCTGCCTTGTCCTCT
NHE2a	
F	AGGAACGCTGCGAAACAT
R	ACGTCCAAGGTCCGAGAA
NHE2b	
F	TGTGGAGCAGCGTGAGTGAA
R	CCTGTGGCCCTCCAGATGAG
NHE2c	
F	CGAGCATCAGACGCAGCATCC
R	GCCGCCACCTTGACTTCTTCTTC
NHE3	
F	GCCTGATGCCTCATAGCC
R	AGCACCCAAAGAAAGACC
NHE5	
F	TTCTCCTTGTCCGCCATTCTGTC
R	AACCGCTGGGAGAAGTGGAACAG
NHE6a	
F	GCTCCTCACCCTCACCATCC
R	AACGCCGTAGATCATCGCCA
NHE6b	
F	ATGGCAACAGCATTCAAACA
R	TAGCAGTGGCAGTCGAGATG
NHE7	
F	CGGAATGGAAGAACTCA
R	CCAGCAAACCGTAAATC
NHE8	
F	ACTTGTTGGTCAGGGTC
R	CTGAAGGGCTTTATGTG
NHE9	
F	TCCTTGGCCTGTTGTCAGAG
R	AGGTGGTGATGGCATGTGTC

Copy numbers of the *NHE* genes in the *L. maculatus* genome were compared with model animals (human, mouse, chicken and zebrafish) and several teleost species (Table 3). Overall, the number of *NHEs* in selected vertebrates varied from nine to twelve. Mammals (human and mouse) had nine *NHE* members (*NHE1*-9), and each *NHE* gene contained only one copy. Chickens possessed 10 *NHE* genes, and two copies of the *NHE2* gene were identified in this genome. Compared with higher vertebrates, *NHEβ* existed only in teleost species, while *NHE4* was missing from all of the fish genomes we investigated. Moreover, the expansions of *NHE2* and *NHE6* genes were common in teleosts. Noticeably, euryhaline fish such as *L. maculatus* and tilapia generated one additional paralogous copy of *NHE2*. The remaining *NHE* members in the *L. maculatus* genome were single-copy.

Twelve *NHE* genes were located on 10 chromosomes of *L. maculatus* (Fig. 1). Two *NHE* genes (*NHEβ* and *NHE3*) were located on chromosome 16 and were positioned on the same scaffold, and *NHE6a* and *NHE2b* were on chromosome 14. The other 8 genes were located on different chromosomes. The multiple copies of genes were distributed on different chromosomes. For example, *NHE2a*, *NHE2b* and *NHE2c* were located on 11, 14 and 24, respectively. *NHE6a* and *NHE6b* were on chromosomes 12 and 14, respectively. The highly homologous *NHE1*

Table 2
The sequence information and accession number of *NHE* family members.

NHE family	mRNA (bp)	ORF (bp)	5′-UTR (bp)	3′-UTR (bp)	Predicted protein (aa)	Molecular weight (kDa)	Isoelectric point (pI)	Domain (aa)	Transmembrane helices	Exon number	Accession number
NHE1	2920	2352	379	189	783	86,559	8.11	78–478	13	12	MF481092
NHE2a	5644	2457	26	3161	818	92,241	8.88	75–475	12	13	MF481093
NHE2b	2160	2160	0	0	719	80,617	8.61	72–471	12	13	MH687073
NHE2c	2812	2442	0	370	813	91,161	8.14	83–483	12	13	MH687074
NHE3	3623	2688	166	769	895	99,090	5.79	115–519	11	16	MF481094
NHE5	2943	2943	0	0	980	107,449	8.13	106–511	10	15	MF481095
NHE6a	5337	2079	321	2937	692	76,837	5.83	65–524	11	16	MH687075
NHE6b	4708	2103	153	2552	700	77,044	6.25	60–519	10	16	MF481096
NHE7	5175	2037	132	3006	678	75,088	5.96	44–503	11	14	MF481097
NHE8	2187	2037	28	122	678	75,802	5.72	158–568	11	9	MF481098
NHE9	2888	1800	17	1071	599	65,373	5.33	17–470	10	16	MF481099
NHEβ	3206	2442	195	569	813	89,887	7.90	85–489	9	12	MF481101

Table 3
Comparison of copy numbers of *NHEs* in several representative vertebrates.

Name	Hum	Mou	Chk	Zbf	Fugu	Mdk	Til	Mac
NHEβ	0	0	0	1	1	1	1	1
NHE1	1	1	1	1	1	1	1	1
NHE2	1	1	2	1	2	2	3	3
NHE3	1	1	1	2	1	1	1	1
NHE4	1	1	1	0	0	0	0	0
NHE5	1	1	1	1	1	1	1	1
NHE6	1	1	1	2	2	2	2	2
NHE7	1	1	1	1	1	1	1	1
NHE8	1	1	1	1	1	1	1	1
NHE9	1	1	1	0	0	1	1	1
Total	9	9	10	10	10	11	12	12

Abbreviations: Hum: human; Mou: mouse; Chk: chicken; Zbf: zebrafish; Mdk: medaka; Til: tilapia; Mac: *L. maculatus*.

and *NHEβ* were detected on chromosomes 7 and 16, respectively.

3.2. Phylogenetic and syntenic analysis

The evolutionary footprints of the *NHE* family among *L. maculatus* and other vertebrates were clearly reappeared by the phylogenetic tree based on the alignments of *NHE* protein sequences. According to the amino acid sequence of each *NHE*, the *NHEs* divided into two separate clades encompassing the plasma membrane isoforms (*NHEβ*, *NHE1-5*) and the intracellular isoforms (*NHE6-9*) (Fig. 2). According to the phylogenic analysis, *NHE8* was considered to be an intracellular *NHE*. The classifications of the respective counterparts, including typical fish species and higher vertebrates, and the evolutionary divergence among them were supported by the robust bootstrap values. Noticeably, it was difficult to distinguish the teleost-specific *NHEβ* from *NHE1* according to the phylogenetic tree.

Owning to the events of teleost-specific whole-genome duplication (WGD), homologous recombination or other complicated evolutionary process, the appearance of paralogous copies originating from the same gene was common. To distinguish these homologous genes, syntenic analysis was chiefly constructed. As shown in Fig. 3, conserved syntenies between *L. maculatus* and other species for *NHE6*,*NHE2* and *NHE1* & *β* indicated the accuracy of related annotations. The orthologous genes were identified and named as *NHE6a*, *NHE6b*, *NHE2a*, *NHE2b*, *NHE2c*, *NHE1* and *NHEβ*. Compared with mammals, gene expansion of *NHE2* and *NHE6* only occurred in tested teleost during the evolution. As shown in Fig. 3A, a conserved downstream synteny was identified for *NHE6a* among *L. maculatus*, human and fugu, whereas the upstream genes were conserved between *L. maculatus* and fugu. For *NHE6b*, the syntenic analysis supported the annotation of *L. maculatus*, which shared similar neighboring genes with fugu. *NHE2a* was located on a conserved genomic region from the mfsd9 to gpr45 genes in all tested organisms (Fig. 3B). Similarly, highly conserved syntenic blocks were found in the genomic region surrounding *NHE2b* between tilapia and *L. maculatus*, demonstrating the veracity of *NHE2b* annotation. For *NHE2c*, the neighboring genes were only conserved in the downstream of *L. maculatus* and tilapia, which may have been due to gene loss or incomplete annotation in the *L. maculatus* genome. It was worth noting that the genomic position of *NHE4* was adjacent to *NHE2* in humans,

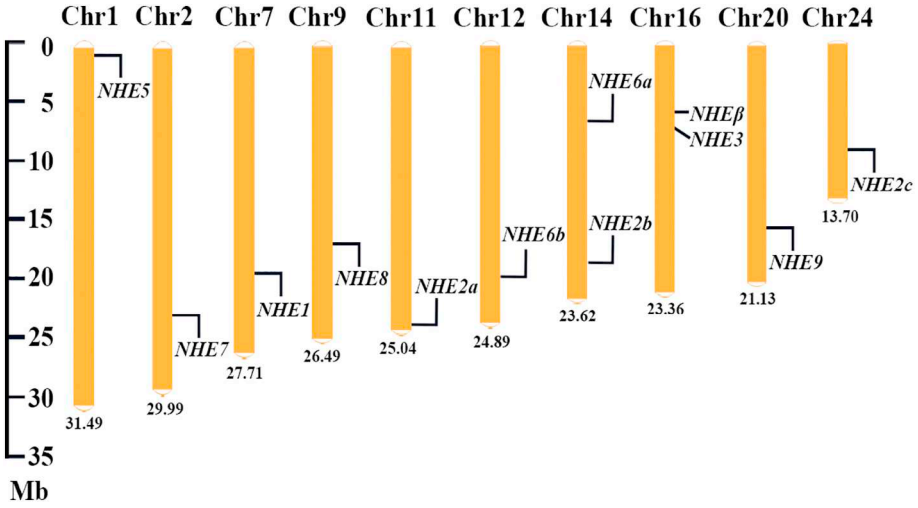

Fig. 1. Chromosome map of the *NHE* genes in *L. maculatus*. Black lines on the bars indicate the locations of each *NHE* gene.

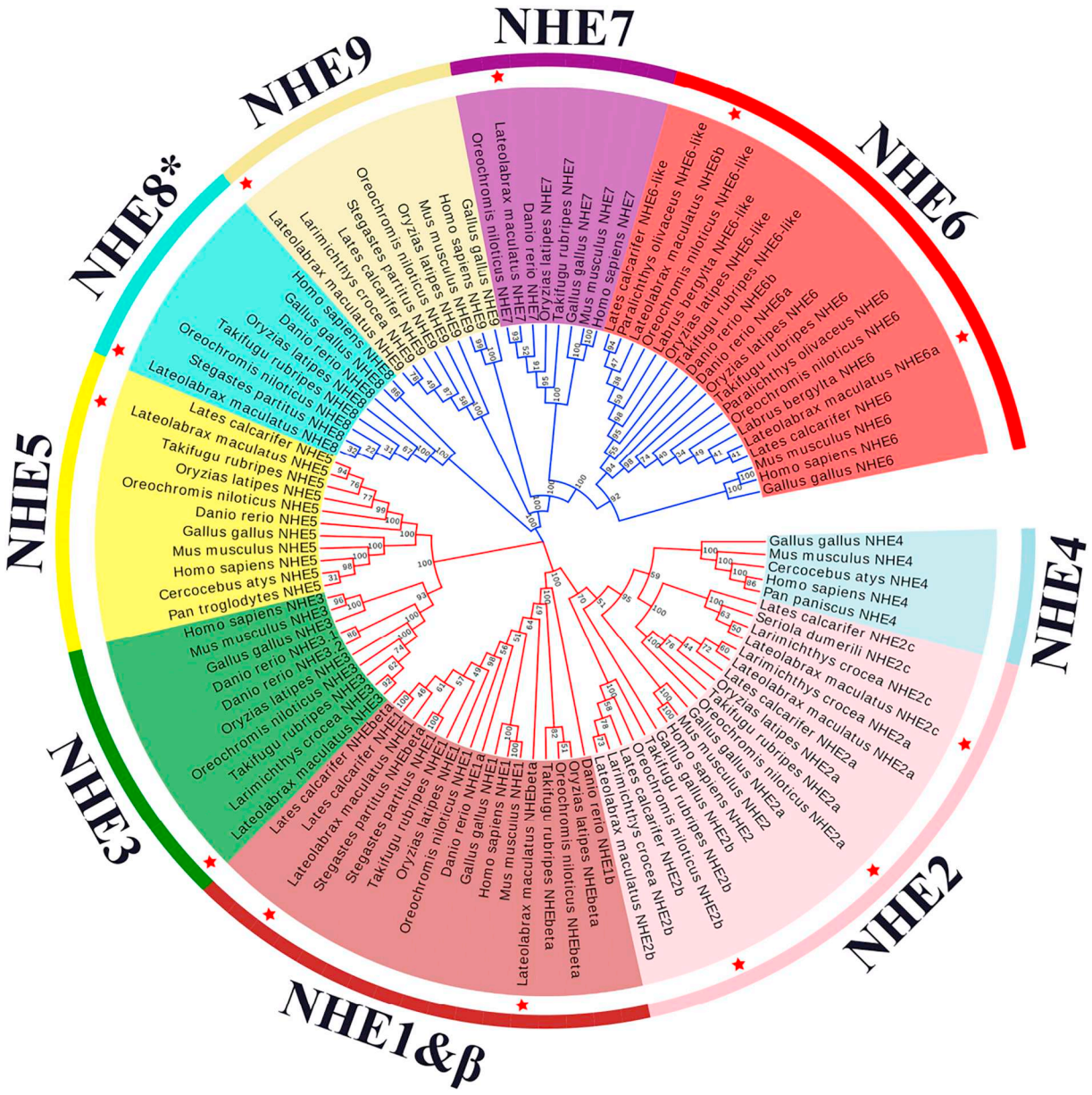

Fig. 2. Phylogenetic analyses of *NHE* proteins from representative vertebrates. The tree was generated with MUSCLE using the neighbor-joining (NJ) method in MEGA 7. Bootstrapping values were indicated by numbers on every node. The red star emphasized each *L. maculatus NHE* gene in this paper.The plasma membrane informs (*NHEβ*, *NHE1–5*), and the intracellular isoforms (*NHE6–9*) were distinguished by red and blue branches. * indicates that *NHE8* also presented at the plasma membrane.

which suggested that *NHE4* in higher vertebrates possibly was generated from the tandem duplication of *NHE2*. Furthermore, a large amount of inversion and loss took place in the upstream genes of *NHE2*, which likely explains the deletion of the *NHE4* gene in teleost. One dramatic but unexpected result was fragmented duplication existed in *NHE1* and *NHEβ* were found in *L. maculatus*, *L. calcarifer*, *T. rubripes* and *O. niloticus* (Fig. 3C), indicting the teleost-specific *NHEβ* might have derived from *NHE1* during WGD, or other evolutionary process.

3.3. Gene structure, conserved domains and motif analysis of the NHE genes

Exon-intron structural analysis can provide additional insights into the evolution of gene families. In Fig. 4, the exon numbers of the 12 *NHE* genes varied from 9 to 16, and *NHE8* and *NHE3* separately owned the minimum and maximum value. These paralog genes (*NHE1*& *NHEβ*, *NHE2a* & *NHE2b* & *NHE2c*, *NHE6a* & *NHE6b*) harbored the same exon numbers, and slight differences were only detected on first, third and sixth exons between *NHE6a* and *NHE6b*. Both compared with *NHE2a*, higher exon identity was found in *NHE2c* than *NHE2b*. The diverse exon-intron structures of *NHEs* may relate to their distinct biological functions.

The conserved homeodomain of Na_H_Exchanger was detected on each of the *NHE* proteins, and few component divergences presented across different members of *NHEs* (Fig. 5). The signal peptide structure was contained by a majority of *NHE* members, except for *NHE6b* and *NHE9*. Furthermore, an additional NEXCam_BD domain adjacent to the end of Na_H_Exchanger was found on *NHEβ*, *NHE1* and *NHE2*.

To further interpret the structural diversity of *NHE* proteins, 12 conserved motifs were identified (Fig. 5). The length of these motifs varied from 21 to 50 amino acids. The motif number among *NHE* genes varied between 6 and 9, while motif 1, motif 2, motif 3, motif 5 and motif 7 can be detected in all *NHE* members. Furthermore, motif 4 and

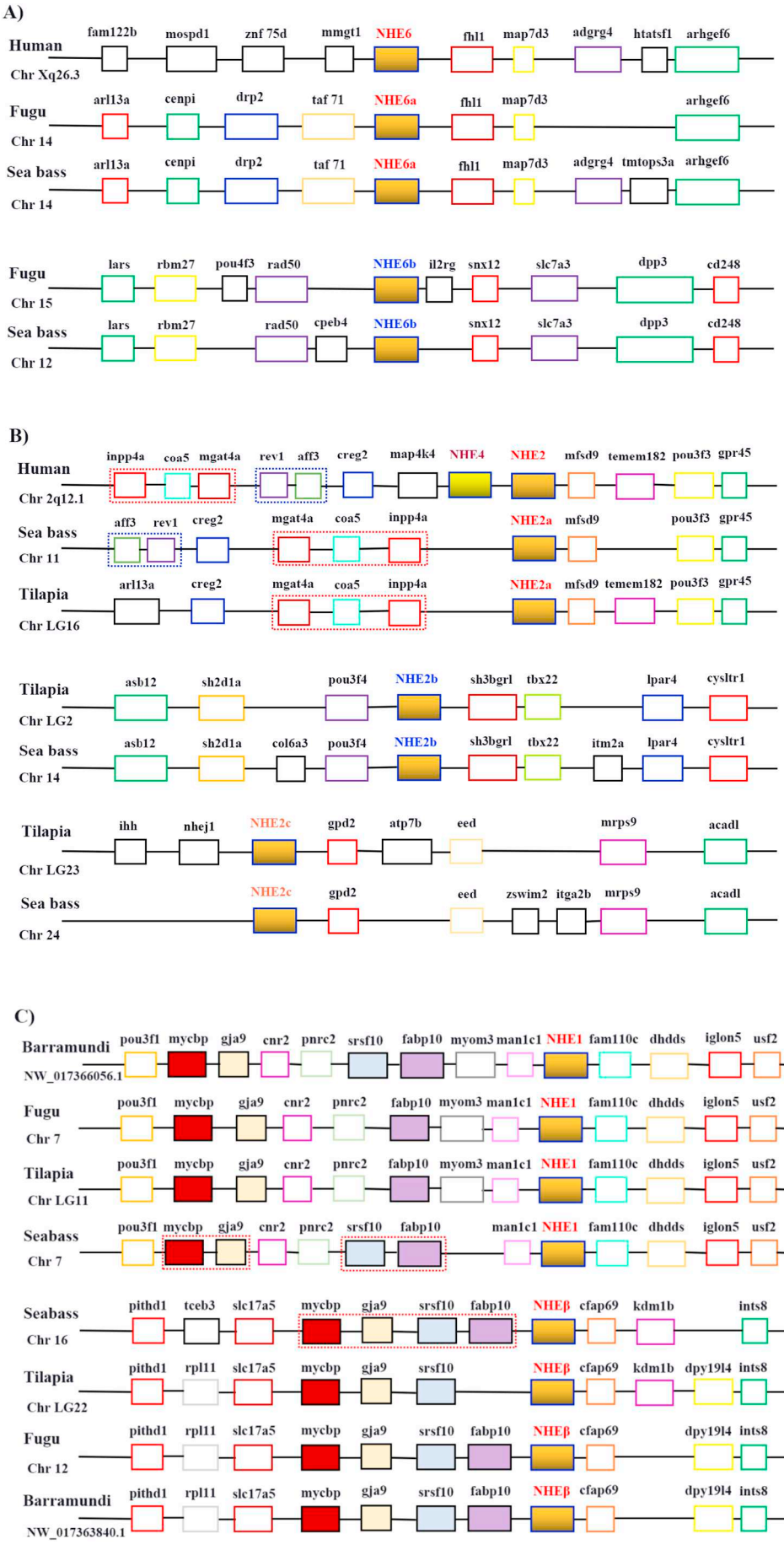

(caption on next page)

Fig. 3. Syntenic analyses of *L. maculatus NHE* genes in selected vertebrates. (A) *NHE6*; (B) *NHE2*; (C) *NHE1* and *NHEβ*. These syntenies were generated with the information obtained from NCBI and Ensembl. The black frame lines represent the member of nonsyntenic genes, and the subject gene is shown highlighted in gold.

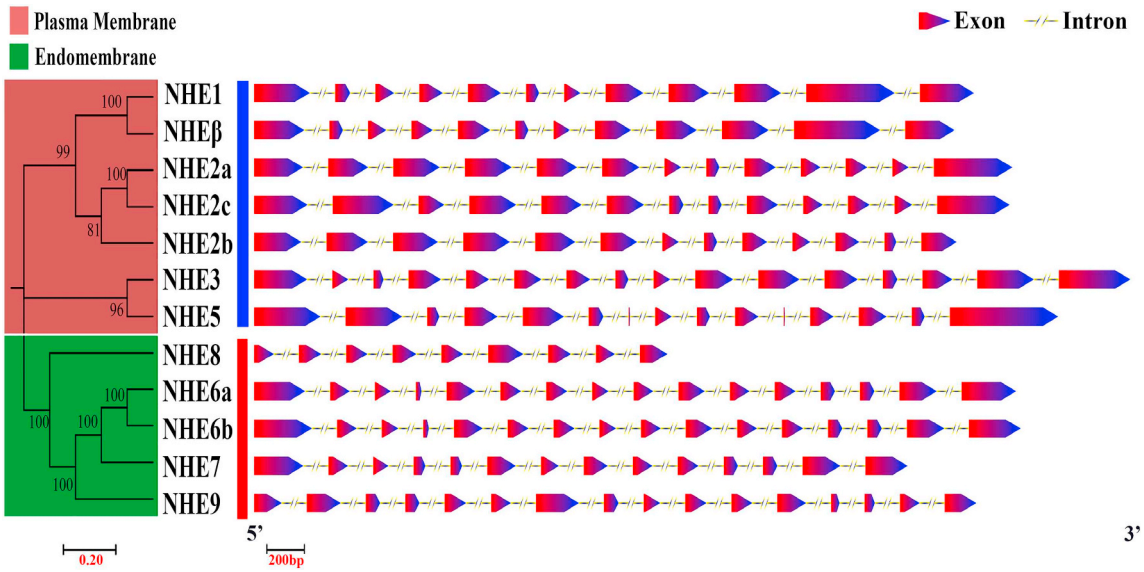

Fig. 4. Phylogenetic and structural analyses of *L. maculatus NHEs*. The *NHE* family was classified into plasma membrane and endomembrane clades based on their phylogenetic relationships. Exon-intron structure analyses were conducted via the GSDS program. Lengths of exons of each *NHE* gene are displayed proportionally according to the scale. Bar = 200 bp.

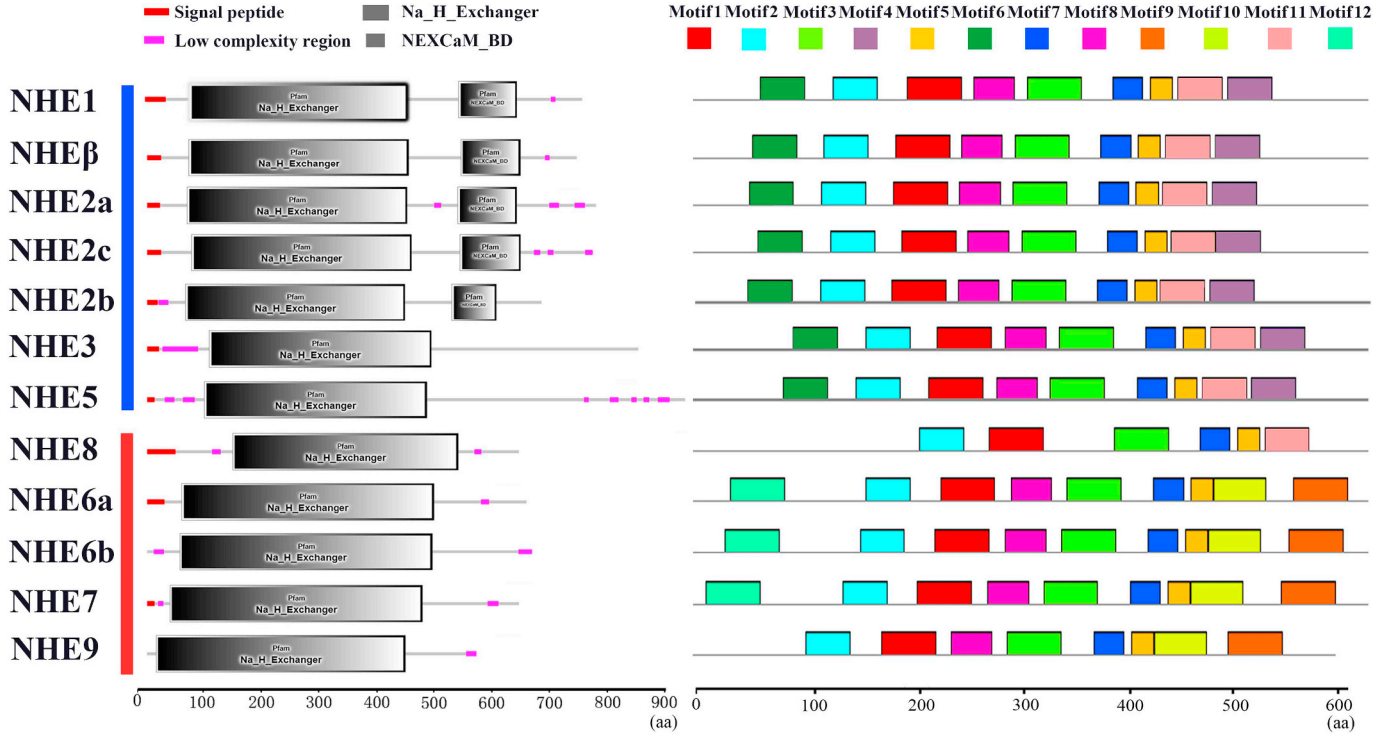

Fig. 5. Homeodomain and motif analyses of *NHEs* proteins. The structure of each *NHE* gene analysis was performed by the SMART analyses service. Twelve typical motifs in the *NHE* proteins were obtained by the MEME database. The width regions of each motif were permitted between 6 and 50 amino acids. Different color blocks represent different motifs.

Fig. 6. Plane view of the *NHEs* TM with total numbers and residues locations. The numbers of TM varied from 9 to 13; *NHEβ* and *NHE1* separately owned the minimum and maximum value. N terminals, C terminals and the directions of membrane helix formation were also correctly presented, among which only *NHE9* formed the first TM from the direction of cytoplasmic to extracellular regions.

motif 6 were found only in plasmalemmal *NHEs* (*NHE1–5*), whereas motif 9 and motif 10 were identified on intracellular *NHEs*, except for *NHE8*. Moreover, motif 11 not only presented on all plasmalemmal *NHEs* but also on *NHE8*. These results may relate to their subcellular localization difference and function diversity between plasmalemmal and intracellular *NHEs*.

3.4. Tertiary structure of NHEs

The numbers of TM varied from 9 to 13 and were mainly concentrated in the range of 10–12. The directions of the first TM usually formed from cytoplasmic to extracellular, with one exception in *NHE9*, in which the direction was the opposite (Fig. 6). The tertiary structure revealed that high proportions of α-helices were presented in all *NHE* members, which varied from 54.7% to 67.0%, whereas β-sheets were found only in *NHE5*, *NHE6* (*NHE6a* & *NHE6b*) and *NHE7*, with 1.3% proportion, while the remaining had random coils at 33.0% to 44.0% (Fig. 7).

3.5. Expression profile analysis of NHE genes

To establish the expression profile of L. *maculatus NHE* genes under normal physiological conditions, qRT-PCR analysis was performed in *L. maculatus* skin, gill, kidney, intestine, liver, stomach, gonad, spleen, heart, brain, muscle and pituitary. The results showed that the tested *NHE* genes exhibited different expression profiles in a tissue-specific manner (Fig. 8). As the main osmoregulatory organ of teleosts, gills had the highest overall expression values of *NHE* genes, and the highest expression level were found in *NHE2c* and *NHE3*, followed by *NHE2a*, *NHE6b* and *NHE8*. In kidney, *NHE3* was the most abundantly expressed

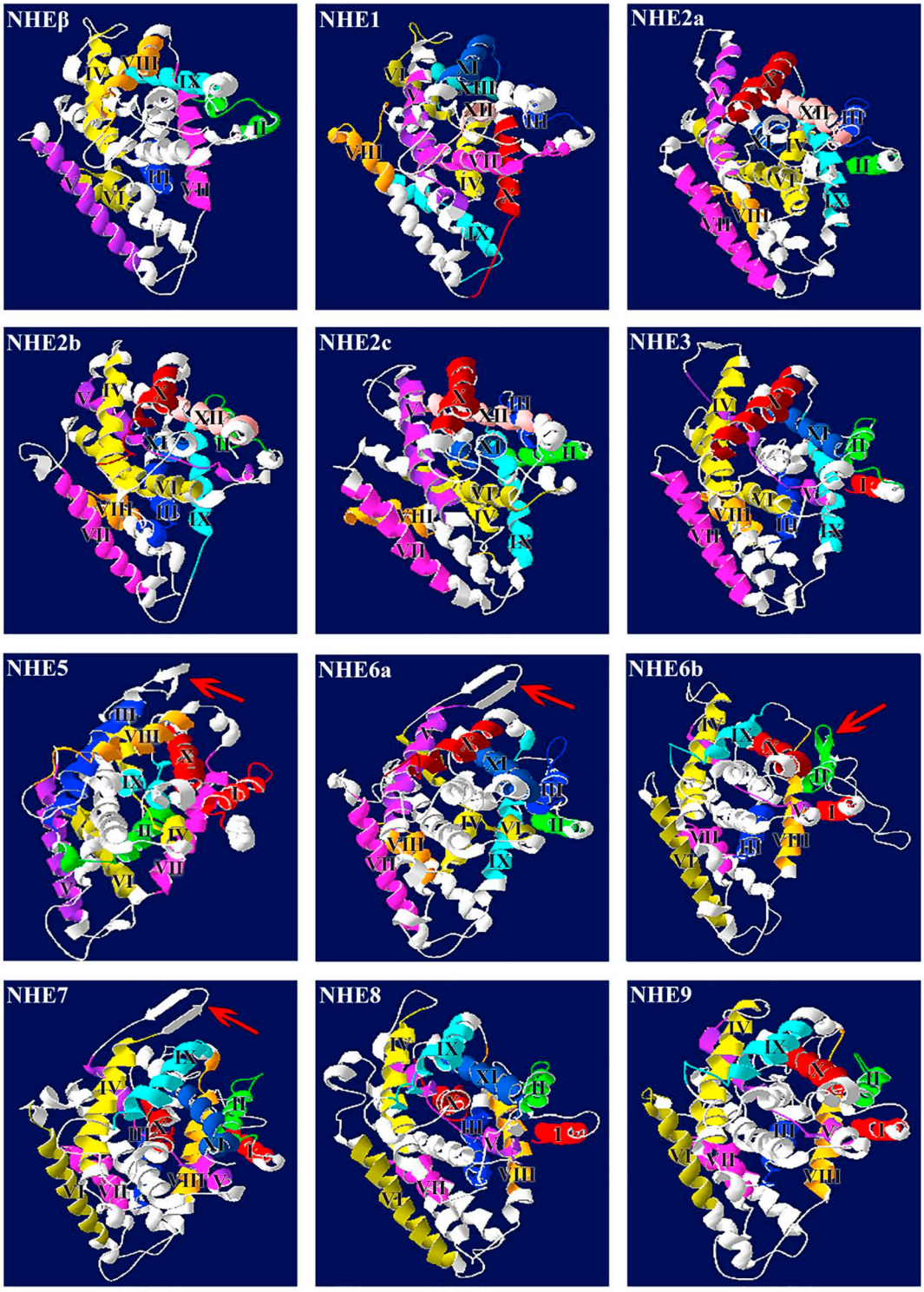

Fig. 7. Comparison of the tertiary structures of *NHE* genes in *L. maculatus*. TM segments are represented by the colored ribbons and are labeled with roman numerals according to the prediction of TMHMM (v.2.0). The remaining segments are reflected by only a gray trace. The tertiary structures of *NHEs* consisted of mostly helices and coils, because the β-sheets were scarce and could be found only in *NHE5*, *NHE6* and *NHE7* in tiny proportions. The β-sheets and the space divergences of *NHE6* are noted with the red arrows.

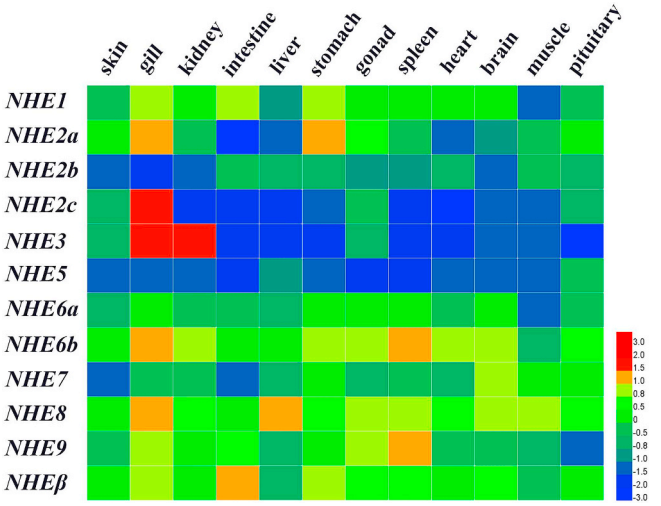

Fig. 8. Heat map of *NHE* genes expression profiles across multiple tissues in *L. maculatus*. The twelve different tissues include skin, gill, kidney, intestine, liver, stomach, gonad, spleen, heart, brain, muscle and pituitary. Each *NHE* gene name is labeled on the left side of the panel. The $\log_{10}$ values of the expressions of *NHE* genes under natural conditions were used for creating the heat map, and the warmer colors indicate the higher expression.

NHE gene. *NHEβ* in the intestine, *NHE2a* in the stomach, *NHE6b* and *NHE9* in the spleen, and *NHE8* in the liver were five of the *NHEs* with relatively higher levels of expression compared with the rest of the tested genes. The opposite trend, in the skin, muscle, gonad, heart, brain and pituitary, all tested 12 *NHE* genes were expressed at modest or relatively low levels, the expressions of several genes were almost undetectable.

3.6. Expression patterns of NHE genes responded to different salinity treatments

To obtain insights into the potential functions of each *NHE* in response to salinity challenge, the expression patterns of *NHEs* of *L. maculatus* were systematically established under different salinity conditions in the gill. In gills (Fig. 9), except for *NHE2b* and *NHE5*, the expression levels of the all *NHEs* were significantly upregulated by low salinity treatment (0 ppt) at the 6 h, while *NHE2c* and *NHE3* were the most strongly induced genes, with 3.7 and 2.2 folds change in expression level, respectively. The high expression induced by freshwater were extended to 12 h, 24 h, or 72 h for *NHE2c*, *NHE3*, *NHE6b*, *NHE7*, *NHE8* and *NHE9*. For isotonic condition (12 ppt), the expressions of *NHE6b*, *NHE8* and *NHE9* were upregulated, by 1.2 to 2.5 folds. Moreover, after high salinity challenge (45 ppt), the expressions of *NHEβ*, *NHE1*, *NHE2a*, *NHE2c*, *NHE3* and *NHE7* were upregulated significantly at 6 h, 12 h or 72 h, on the contrary, the downregulated expressions were detected in *NHE2c*, *NHE3*, *NHE6a*, *NHE6b*, *NHE8* and *NHE9* at different time point after 12 h.

4. Discussion

NHEs, as ubiquitous ion transporters, were detected from prokaryotes to eukaryotes and are chiefly regulators of the concentration gradients of Na (+) and H (+) for electroneutral exchange, thereby assuming crucial biological functions in pharmacological and physiological processes (Orlowski and Grinstein, 2004). In this paper, the identification and characterization of the *NHE* gene family was first established in *L. maculatus*; subsequently, its expression patterns encountering different salinity challenges were also evaluated by qRT-PCR analysis.

A complete repertoire of 12 Na^+/H^+ exchangers (*NHEs*) was identified in the *L. maculatus* genome, including *NHEβ*, *NHE1*, *NHE2a*, *NHE2b*, *NHE2c*, *NHE3*, *NHE5*, *NHE6a*, *NHE6b*, *NHE7*, *NHE8* and *NHE9*. Among them, *NHE5* extracted from the *L. maculatus* transcriptome library and genome was first presented in a partial sequence, which was then completed by the sequencing technology. Maybe the failure of getting the full-length sequence of *NHE5* was attributed to its lower endogenous expression level (Mackinder et al., 2017). The gene structure analysis failed to find differences in the exon number in multiple copies and homologous genes, which further highlighted the conserved evolution among them (L. Zhang et al., 2017). The protein structures of *NHEs* generally consisted of a signal peptide, the Na_H_Exchanger domain and some TMs. The Na_H_Exchanger domain was detected in all *NHEs* of *L. maculatus*, which should be considered to be a classification standard for unknown *NHE* targets (Wu et al., 2016).

The numbers of TM in *L. maculatus NHEs* varied from 9 to 13, which was in line with previous results (Zizak et al., 2000; Kondapalli et al., 2014). The extreme TM values and space divergences were considered to be the basis by which to distinguish the highly homologous *NHEβ* and *NHE1*. The results of higher α-helices and scarcer β-sheet distributions were also revealed by previous *NHE1* studies (Emily et al., 2007). The conformational divergences associated with the ion movements (Hunte et al., 2005) can also be detected on the corresponding tertiary structure regions.

The evolution and expansion of *NHEs* in *L. maculatus* and other vertebrates were revealed by the analysis of the copy numbers. The reasons for the *NHE* number divergences were summarized as two key factors; the duplication in some *NHE* genes and the inherent existence of species-specific *NHEs*. Notably, the copy numbers of *NHE* genes in mammalian (human and mouse) genomes were relatively conserved and had only one copy. However, two copies of the *NHE2* gene were detected in the chicken genome. Furthermore, the third copy of gene *NHE2c* was identified in euryhaline teleosts, such as *O. mossambicus* and *L. maculatus*. Therefore, the evolutionary traces of the genes were indirectly reflected by the copy divergences. The *NHE4* gene was detected solely in terrestrial animals, which conflicted with the study of Brett's (Brett et al., 2005). Instead, *NHEβ* was present only in fish species, suggesting that the above *NHE* genes were actively obtained or discarded during the evolution process (Xie et al., 2015). Furthermore, as the oldest *NHE* gene (Brett et al., 2005), *NHE9* was missing in some fish.

The strong bootstrap supported linking *L. maculatus NHEs* to their respective homologs in well-described model animals (human, mouse, chicken and zebrafish), allowed us to confidently identify their orthologous relationships by phylogenetic analysis. The present results were consistent with and more comprehensive than the previous study on zebrafish *NHEs* family (Yan et al., 2007). Furthermore, the conserved motif and gene structure analyses also supported the phylogenetic classification of *L. maculatus NHEs*. The unique subcellular distributions of *NHE8* were appropriately explained by its detached branch and specific motif compositions (Ohgaki et al., 2011). For multiple copy genes of *NHE6*, *NHE2* and the homologous genes of *NHE1* & *NHEβ*, the syntenic analyses were applied for their proper annotation. Relying on the adjacent genomic position and the close phylogenetic relationship, we deduced that the *NHE4* gene possibly was produced by tandem duplication of the *NHE2* gene (Brett et al., 2005). Simultaneously, the loss of teleost *NHE4* possibly was induced by large extent inversions and losses, which took place in the *NHE2a* gene nearby. Furthermore, the opinion that fish *NHEβ* originated from its homologous gene *NHE1* (Rimoldi et al., 2009) was supported by the segmental duplication that occurred in the synteny maps of *L. maculatus*, barramundi, fugu and tilapia. In total, the lineage-specific gene expansions of *L. maculatus NHEs* were modestly explicated by the tandem duplications, segmental duplications and whole genome duplications (Aparicio et al., 2002; Jaillon et al., 2004).

Regarding tissue-specific expression profiles, only a limited number of *NHEs* were highly expressed in 12 different tissues of *L. maculatus*. However, *NHE2c* and *NHE3* might be the exception to this, because they

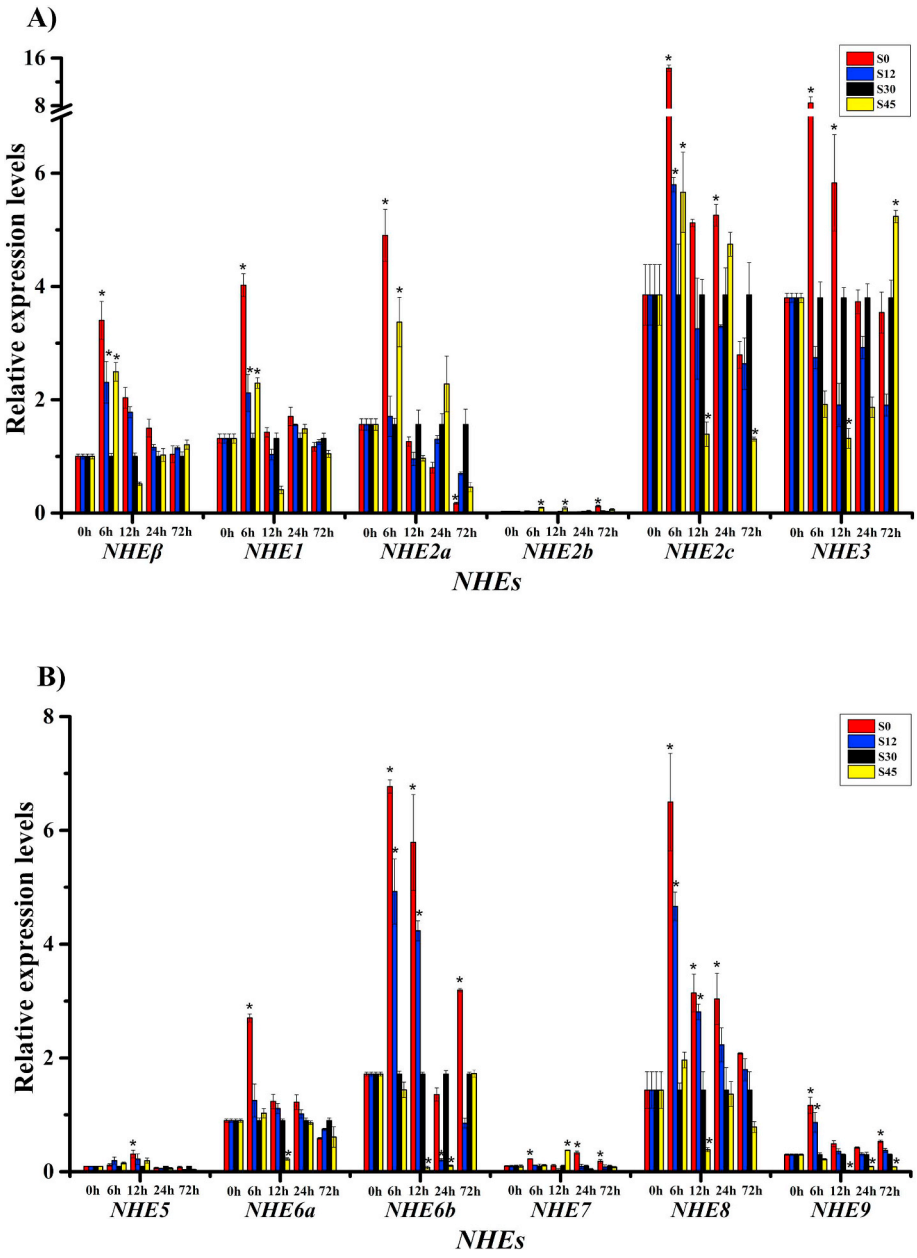

Fig. 9. Expression patterns of *NHE* genes in gills responding to different salinity challenges at every time point. (A) *NHEβ*, *1–3*; (B) *NHE5–9*. The quantitative RT-PCR method was used for determining the expressions of gills under four salinity treatments (0 ppt, 12 ppt, 30 ppt and 45 ppt) and the samples were run in triplicate. According to the comparative $2^{-\Delta\Delta CT}$ method, *18S* mRNA was used as the internal control and transcript level of *NHEβ* in S30 at 0 h was arbitrarily set to 1, subsequently the levels in other *NHEs* were given relative to this. The x-Axis provided the names of involved genes and each sampling time. Significant differences were noted by different letters in each *NHE* gene ($P < 0.05$).

were expressed at relatively high levels at the main osmoregulatory organ of the gill and kidney. This suggests that *NHE2c* and *NHE3* are essential transport proteins that played crucial roles in *L. maculatus* growth and development. Previous studies reported that SLC9A had multiple functions involvement in ion transport of vertebrate, knockout of NHE2 in mice lack an overt renal or gastrointestinal phenotype. NHE3 knockout mice also displayed the defects for sodium and water reabsorption in both intestinal and renal tubular epithelia (Ledoussal et al., 2001a; Ledoussal et al., 2001b). Interestingly, the absence of NHE2 apparently can be compensated for via NHE3 upregulation (Gawenis et al., 2002; Bachmann et al., 2004). Thereby, *NHE2* and *NHE3* generally were considered as focused genes in fish, to explore their roles in pH homeostasis, osmoregulation and ammonia excretion.

The complicated physiological and metabolic activities involving growth, development and reproduction of fish were closely correlated with the abiotic factors of salinity (X. Zhang et al., 2017). For *L. maculatus* expression patterns, the higher expression levels were reflected on *NHE2a*, *NHE2c*, *NHE3*, *NHE6b* and *NHE8* under low salinity (0 ppt) stress, while *NHE2c* and *NHE3* were the most strongly induced genes. Similarly, the mRNA expressions of *NHE2c* and *NHE3* in the marine fish, longhorn sculpin (*Myoxocephalus octodecemspinosus*), were upregulated in gills in exposing to a salinity of 20 ppt, and the expression level of *NHE2b* was also undetectable during acclimating to 10 ppt salinity (Hyndman et al., 2009). As expanded genes, *NHE2c* and *NHE6b* had notably high expression levels compared with other homologous copies in the same gene. Therefore, they should be considered as candidate genes for subsequently biological studies. The results showed that most *NHEs* were dramatically upregulated by freshwater stress, which were consistent with previous studies (Scott and Schulte, 2005; Gibbons et al., 2018). Contrastingly, the significantly downregulated expressions caused by the high salinity of 45 were also detected in *NHE2c*, *NHE3*, *NHE6a*, *NHE6b*, *NHE8* and *NHE9*. The above results reflected the biological function of *NHEs* in the exchange of extracellular sodium for intracellular protons, to maintain the homeostasis of organisms. After transferring from seawater (SW) to fresh water (FW) in Japanese sea bass (*L. japonicus*), the mRNA expression levels in the gills of *NHE3* were upregulated for maintaining ionic balance. Moreover, SW-type ionocytes (also known as chloride cells or mitochondrion-rich

cells) also transformed into FW-type *NHE3* ionocytes in the gills for ion uptake, and migrated their distribution from filaments to lamellae during FW adaptation (Inokuchi et al., 2017). Pharmacological evidence of EIPA (NHE-specific inhibitor) indicated *F. heteroclitus* relied solely on *NHE2* for Na^+ transport across the apical membrane of ionocytes acclimated to freshwater (Brix et al., 2018). Furthermore, *NHE2* and *NHE3* also function together to enable H^+ secretion and bicarbonate reclamation in seawater-acclimated medaka (Liu et al., 2016).

In addition, the expression variations in the salinity 12 group were more modest and stable than those of other treatments. It is possible that salinity 12 was close to the isosmotic point of *L. maculatus*, which decreased the extra energy consumption and enhanced related resistance (Nursanti et al., 2017). Researching these high expression patterns of *NHE* will contribute to the exploration of related biological functions that are involved in the survival and growth of *L. maculatus*.

5. Conclusions

In this study, the entire *NHE* gene family, including 12 *NHE* members, was systematically identified in the *L. maculatus* genome, which was further supported by the phylogenetic, syntenic, and gene structures analysis. *L. maculatus NHEs* exhibited gene-specific expression patterns under normal physiological conditions or after acute salinity challenge. The notably highly expression levels of *NHE2c* and *NHE3* both in normal and salinity challenged conditions suggesting their potential involvement in osmotic regulation and salinity adaptation. These studies may set the foundation for future study on the stress physiology and molecular mechanism of salinity acclimation and osmoregulation in teleost.

Supplementary data to this article can be found online at https://doi.org/10.1016/j.cbd.2019.01.001.

Conflict of interest

The authors have no conflicts of interest to declare.

Acknowledgements

This study was funded by National Key R&D Program of China (2018YFD0900101); National Natural Science Foundation of China (31602147) and Agriculture Research System of China (CARS-47).

References

Aparicio, S., Chapman, J., Stupka, E., Putnam, N., Jer-ming, C., Dehal, P., Christoffels, A., Rash, S., Hoon, S., Smit, A., Sollewijn Gelpke, M.D., Roach, J., Oh, T., Ho, I.Y., Wong, M., Detter, C., Verhoef, F., Predki, P., Tay, A., 2002. Whole-genome shotgun assembly and analysis of the genome of Fugu rubripes. Science 297, 1301–1310.

Bachmann, O., Riederer, B., Rossmann, H., Groos, S., Schultheis, P.J., Shull, G.E., Gregor, M., Manns, M.P., Seidler, U., 2004. The Na^+/H^+ exchanger isoform 2 is the predominant NHE isoform in murine colonic crypts and its lack causes NHE3 upregulation. Am. J. Physiol. Gastrointest. Liver Physiol. 287, G125.

Brett, C.L., Donowitz, M., Rao, R., 2005. Evolutionary origins of eukaryotic sodium/proton exchangers. Am. J. Phys. Cell Phys. 288, C223–C239.

Brix, K.V., Brauner, C.J., Schluter, D., Wood, C.M., 2018. Pharmacological evidence that DAPI inhibits NHE2 in *Fundulus heteroclitus* acclimated to freshwater. Comp. Biochem. Physiol. C 211 (1–6).

Brown, P., Baxter, L., Hickman, R., Beynon, J., Moore, J.D., Ott, S., 2013. MEME-LaB: motif analysis in clusters. Bioinformatics 29, 1696–1697.

Capasso, G., Cantone, A., Evangelista, C., Zacchia, M., Trepiccione, F., Acone, D., Rizzo, M., 2005. Channels, carriers, and pumps in the pathogenesis of sodium-sensitive hypertension. Semin. Nephrol. 25, 419–424.

Choe, K.P., Kato, A., Hirose, S., Plata, C., Sindić, A., Romero, M.F., Claiborne, J.B., Evans, D.H., 2005. NHE3 in an ancestral vertebrate: primary sequence, distribution, localization, and function in gills. Am. J. Phys. Regul. Integr. Comp. Phys. 289, R1520–R1534.

Donowitz, M., Ming Tse, C., Fuster, D., 2013. SLC9/NHE gene family, a plasma membrane and organellar family of Na^+/H^+ exchangers. Mol. Asp. Med. 34, 236–251.

Edgar, R.C., 2004. MUSCLE: multiple sequence alignment with high accuracy and high throughput. Nucleic Acids Res. 32, 1792–1797.

Emily, R.S., Jan, K.R., Brian, D.S., Larry, F., 2007. Structural and functional analysis of the Na^+/H^+ exchanger. Biochem. J. 401, 623–633.

Fuster, D.G., Alexander, R.T., 2014. Traditional and emerging roles for the SLC9 Na^+/H^+ exchangers. Pflugers Arch. 466, 61–76.

Gasteiger, E., Gattiker, A., Hoogland, C., Ivanyi, I., Appel, R.D., Bairoch, A., 2003. ExPASy: the proteomics server for in-depth protein knowledge and analysis. Nucleic Acids Res. 31, 3784–3788.

Gawenis, L.R., Stien, X., Shull, G.E., Schultheis, P.J., Woo, A.L., Walker, N.M., Clarke, L.L., 2002. Intestinal NaCl transport in NHE2 and NHE3 knockout mice. Am. J. Physiol. Gastrointest. Liver Physiol. 282, G776.

Gibbons, T.C., McBryan, T.L., Schulte, P.M., 2018. Interactive effects of salinity and temperature acclimation on gill morphology and gene expression in threespine stickleback. Comp. Biochem. Physiol. A Physiol. 221, 55–62.

Goyal, S., Vanden Heuvel, G., Aronson, P.S., 2003. Renal expression of novel Na^+/H^+exchanger isoform NHE8. Am. J. Phys. Renal Phys. 284, F467–F473.

Guffey, S.C., Fliegel, L., Goss, G.G., 2015. Cloning and characterization of Na + /H + exchanger isoforms NHE2 and NHE3 from the gill of Pacific dogfish *Squalus suckleyi*. Comp. Biochem. Physiol. B 188, 46–53.

Harter, T.S., May, A.G., Federspiel, W.J., Supuran, C.T., Brauner, C.J., 2018. Time course of red blood cell intracellular pH recovery following short-circuiting in relation to venous transit times in rainbow trout, *Oncorhynchus mykiss*. Am. J. Phys. Regul. Integr. Comp. Phys. 315, R397–R407.

Howe, K., Clark, M.D., Torroja, C.F., Torrance, J., Berthelot, C., Muffato, M., Collins, J.E., Humphray, S., McLaren, K., Matthews, L., McLaren, S., Sealy, I., Caccamo, M., Churcher, C., Scott, C., Barrett, J.C., Koch, R., Rauch, G.-J., White, S., Chow, W., 2013. The zebrafish reference genome sequence and its relationship to the human genome. Nature 496, 498–503.

Hu, B., Jin, J., Guo, A.-Y., Zhang, H., Luo, J., Gao, G., 2015. GSDS 2.0: an upgraded gene feature visualization server. Bioinformatics 31, 1296–1297.

Hua, X., Rongji, C., Ghishan, F.K., 2005. Subcloning, localization, and expression of the rat intestinal sodium-hydrogen exchanger isoform 8. Am. J. Phys. Gastrointest. Liver 52, G36–G41.

Hunte, C., Screpanti, E., Venturi, M., Rimon, A., Padan, E., Michel, H., 2005. Structure of a Na^+/H^+ antiporter and insights into mechanism of action and regulation by pH. Nature 435, 1197–1202.

Hwang, P.-P., Lee, T.-H., 2007. New insights into fish ion regulation and mitochondrion-rich cells. Comp. Biochem. Physiol. A Mol. Integr. Physiol. 148, 479–497.

Hwang, P.-P., Lee, T.-H., Lin, L.-Y., 2011. Ion regulation in fish gills: recent progress in the cellular and molecular mechanisms. Am. J. Phys. Regul. Integr. Comp. Phys. 301, R28–R47.

Hyndman, K.A., Edwards, S.L., Kratochvilova, H., Claiborne, J.B., Evans, D.H., 2009. The effect of short-term, low-salinity acclimation on gill NHE, AE1 and HAT expression in the longhorn sculpin, *Myoxocephalus octodecemspinosus*. FASEB J. 23, 778.717.

Inokuchi, M., Nakamura, M., Miyanishi, H., Hiroi, J., Kaneko, T., 2017. Functional classification of gill ionocytes and spatiotemporal changes in their distribution after transfer from seawater to freshwater in Japanese seabass. J. Exp. Biol. 220, 4720.

Ivanis, G., Braun, M., Perry, S.f., 2008a. Renal expression and localization of SLC9A3 sodium/hydrogen exchanger and its possible role in acid-base regulation in freshwater rainbow trout (*Oncorhynchus mykiss*). Am. J. Phys. Regul. Integr. Comp. Phys. 295, R971.

Ivanis, G., Esbaugh, A.J., Perry, S.F., 2008b. Branchial expression and localization of SLC9A2 and SLC9A3 sodium/hydrogen exchangers and their possible role in acid–base regulation in freshwater rainbow trout (*Oncorhynchus mykiss*). J. Exp. Biol. 211, 2467.

Jaillon, O., Aury, J.-M., Brunet, F., Petit, J.-L., Stange-Thomann, N., Mauceli, E., Bouneau, L., Fischer, C., Ozouf-Costaz, C., Bernot, A., Nicaud, S., Jaffe, D., Fisher, S., Lutfalla, G., Dossat, C., Segurens, B., Dasilva, C., Salanoubat, M., Levy, M., Boudet, N., 2004. Genome duplication in the teleost fish *Tetraodon nigroviridis* reveals the early vertebrate proto-karyotype. Nature 431, 946–957.

Kasahara, M., Naruse, K., Sasaki, S., Nakatani, Y., Wei, Q., Ahsan, B., Yamada, T., Nagayasu, Y., Doi, K., Kasai, Y., Jindo, T., Kobayashi, D., Shimada, A., Toyoda, A., Kuroki, Y., Fujiyama, A., Sasaki, T., Shimizu, A., Asakawa, S., Shimizu, N., 2007. The medaka draft genome and insights into vertebrate genome evolution. Nature 447, 714–719.

Kondapalli, K.C., Prasad, H., Rao, R., 2014. An inside job: how endosomal Na^+/H^+ exchangers link to autism and neurological disease. Front. Cell. Neurosci. 8, 172.

Krogh, A., Larsson, B., von Heijne, G., Sonnhammer, E.L.L., 2001. Predicting transmembrane protein topology with a hidden markov model: application to complete genomes11Edited by F. Cohen. J. Mol. Biol. 305, 567–580.

Kumar, S., Stecher, G., Tamura, K., 2016. MEGA7: molecular evolutionary genetics analysis version 7.0 for bigger datasets. Mol. Biol. Evol. 33, 1870–1874.

Ledoussal, C., Lorenz, J.N., Nieman, M.L., Soleimani, M., Schultheis, P.J., Shull, G.E., 2001a. Renal salt wasting in mice lacking NHE3 Na^+/H^+ exchanger but not in mice lacking NHE2. Am. J. Physiol. Ren. Physiol. 281, F718.

Ledoussal, C., Woo, A.L., Miller, M.L., Shull, G.E., 2001b. Loss of the NHE2 Na(+)/H(+) exchanger has no apparent effect on diarrheal state of NHE3-deficient mice. Am. J. Physiol. Gastrointest. Liver Physiol. 281, G1385.

Letunic, I., Doerks, T., Bork, P., 2012. SMART 7: recent updates to the protein domain annotation resource. Nucleic Acids Res. 40, D302–D305.

Li, S., Kato, A., Takabe, S., Chen, A.P., Michael, F.R., Umezawa, T., Nakada, T., Hyodo, S., Hirose, S., 2013. Expression of a novel isoform of Na^+/H^+ exchanger 3 in the kidney and intestine of banded houndshark, *Triakis scyllium*. Am. J. Phys. Regul. Integr. Comp. Phys. 304, R865–R876.

Liu, S.-T., Horng, J.-L., Chen, P.-Y., Hwang, P.-P., Lin, L.-Y., 2016. Salt secretion is linked to acid-base regulation of ionocytes in seawater-acclimated medaka: new insights into the salt-secreting mechanism. Sci. Rep. 31433.

Mackinder, L.C.M., Chen, C., Leib, R.D., Patena, W., Blum, S.R., Rodman, M., Ramundo, S., Adams, C.M., Jonikas, M.C., 2017. A spatial Interactome reveals the protein

organization of the algal CO_2-concentrating mechanism. Cell 171, 133–147 (e114).
Malo, M.E., Fliegel, L., 2006. Physiological role and regulation of the Na^+/H^+ exchanger. Can. J. Physiol. Pharmacol. 84, 1081–1095.
Mulder, N., Apweiler, R., 2007. InterPro and InterProScan: tools for protein sequence classification and comparison. Methods Mol. Biol. 396, 59–70.
Musch, M.W., Arvans, D.L., Wu, G.D., Chang, E.B., 2009. Functional coupling of the downregulated in adenoma Cl^-/base exchanger DRA and the apical Na^+/H^+ exchangers NHE2 and NHE3. Am. J. Physiol. Gastrointest. Liver Physiol. 296, G202–G210.
N, G., MC, P., 1997. SWISS-MODEL and the Swiss-PdbViewer: an environment for comparative protein modeling. Electrophoresis 18, 2714–2723.
Nursanti, L., Nofitasari, E., Hayati, A., Hariyanto, S., Irawan, B., Soegianto, A., 2017. Effects of cadmium on metallothionein and histology in gills of tilapia (*Oreochromis niloticus*) at different salinities. Toxicol. Environ. Chem. 1-12.
Ohgaki, R., van Ijzendoorn, S.C.D., Matsushita, M., Hoekstra, D., Kanazawa, H., 2011. Organellar Na^+/H^+ exchangers: novel players in organelle pH regulation and their emerging functions. Biochemistry 50, 443–450.
Orlowski, J., Grinstein, S., 2004. Diversity of the mammalian sodium/proton exchanger SLC9 gene family. Pflugers Arch. - Eur. J. Physiol. 447, 549–565.
Reilly, B.D., Cramp, R.L., Wilson, J.M., Campbell, H.A., Franklin, C.E., 2011. Branchial osmoregulation in the euryhaline bull shark, *Carcharhinus leucas*: a molecular analysis of ion transporters. J. Exp. Biol. 214, 2883.
Rimoldi, S., Terova, G., Brambilla, F., Bernardini, G., Gornati, R., Saroglia, M., 2009. Molecular characterization and expression analysis of Na^+/H^+ exchanger (NHE)-1 and c-Fos genes in sea bass (*Dicentrarchus labrax*, L) exposed to acute and chronic hypercapnia. J. Exp. Mar. Biol. Ecol. 375, 32–40.
Rummer, J.L., Roshan-Moniri, M., Balfry, S.K., Brauner, C.J., 2010. Use it or lose it? Sablefish, *Anoplopoma fimbria*, a species representing a fifth teleostean group where the βNHE associated with the red blood cell adrenergic stress response has been secondarily lost. J. Exp. Biol. 213, 1503.
Scott, G.R., Schulte, P.M., 2005. Intraspecific variation in gene expression after seawater transfer in gills of the euryhaline killifish *Fundulus heteroclitus*. Comp. Biochem. Physiol. A Mol. Integr. Physiol. 141, 176–182.
Tine, M., Kuhl, H., Gagnaire, P.-A., Louro, B., Desmarais, E., Martins, R.S.T., Hecht, J., Knaust, F., Belkhir, K., Klages, S., Dieterich, R., Stueber, K., Piferrer, F., Guinand, B., Bierne, N., Volckaert, F.A.M., Bargelloni, L., Power, D.M., Bonhomme, F., Canario, A.V.M., Reinhardt, R., 2014. European sea bass genome and its variation provide insights into adaptation to euryhalinity and speciation. Nat. Commun. 5770.
Wagner, C.A., Finberg, K.E., Breton, S., Marshansky, V., Brown, D., Geibel, J.P., 2004. Renal Vacuolar H^+-ATPase. Physiol. Rev. 84, 1263–1314.
Watanabe, S., Niida, M., Maruyama, T., Kaneko, T., 2008. Na^+/H^+ exchanger isoform 3 expressed in apical membrane of gill mitochondrion-rich cells in Mozambique tilapia *Oreochromis mossambicus*. Fish. Sci. 74, 813–821.
Wu, M., Li, Y., Chen, D., Liu, H., Zhu, D., Xiang, Y., 2016. Genome-wide identification and expression analysis of the IQD gene family in moso bamboo (*Phyllostachys edulis*). Sci. Rep. 6, 24520.
Xie, Y., Song, L., Weng, Z., Liu, S., Liu, Z., 2015. Hsp90, Hsp60 and sHsp families of heat shock protein genes in channel catfish and their expression after bacterial infections. Fish Shellfish Immunol. 44, 642–651.
Yan, J.-J., Chou, M.-Y., Kaneko, T., Hwang, P.-P., 2007. Gene expression of Na^+/H^+ exchanger in zebrafish H^+-ATPase-rich cells during acclimation to low-Na^+ and acidic environments. Am. J. Phys. Cell Phys. 293, C1814–C1823.
Zhang, L., Zhao, J., Feng, C., Liu, M., Wang, J., Hu, Y., 2017. Genome-wide identification, characterization of the MADS-box gene family in Chinese jujube and their involvement in flower development. Sci. Rep. 6, 24520.
Zhang, X., Wen, H., Wang, H., Ren, Y., Zhao, J., Li, Y., 2017. RNA-Seq analysis of salinity stress–responsive transcriptome in the liver of spotted sea bass (*Lateolabrax maculatus*). PLoS One 12, 1–18.
Zizak, M., Cavet, M.E., Bayle, D., Tse, C.-M., Hallen, S., Sachs, G., Donowitz, M., 2000. Na^+/H^+ exchanger NHE3 has 11 membrane spanning domains and a cleaved signal peptide: topology analysis using in vitro transcription/translation. Biochemistry 39, 8102–8112.